

Signals of the QCD phase transition in core-collapse supernovae

I. Sagert, M. Hempel, G. Pagliara and J. Schaffner-Bielich*

Institute for Theoretical Physics, Goethe University, Max-von-Laue-Str. 1, 60438 Frankfurt am Main, Germany

**Institute for Theoretical Physics, Ruprecht-Karls-University, Philosophenweg 16, D-69120 Heidelberg, Germany*

T. Fischer[†], A. Mezzacappa[‡], F.-K. Thielemann[†] and M. Liebendörfer[†]

[†]*Department of Physics, University of Basel, Klingelbergstr. 82, 4056 Basel, Switzerland*

[‡]*Physics Division, Oak Ridge National Laboratory, Oak Ridge, TN 37831*

(Dated: October 30, 2018)

We explore the implications of the QCD phase transition during the postbounce evolution of core-collapse supernovae. Using the MIT bag model for the description of quark matter and assuming small bag constants, we find that the phase transition occurs during the early postbounce accretion phase. This stage of the evolution can be simulated with general relativistic three-flavor Boltzmann neutrino transport. The phase transition produces a second shock wave that triggers a delayed supernova explosion. If such a phase transition happens in a future galactic supernova, its existence and properties should become observable as a second peak in the neutrino signal that is accompanied by significant changes in the energy of the emitted neutrinos. In contrast to the first neutronization burst, this second neutrino burst is dominated by the emission of anti-neutrinos because the electron-degeneracy is lifted when the second shock passes through the previously neutronized matter.

PACS numbers: 12.38.-t 12.38.Mh 21.65.Qr 25.75.Nq 26.30.-k 26.50.+x 26.60.-c 26.60.Kp 95.30.Sf 95.55.Vj 95.85.Ry 97.60.Bw

In search of the phase transition from hadronic to deconfined matter, heavy ion experiments at RHIC and at LHC at CERN explore the QCD phase diagram for large temperatures and small baryochemical potentials. For these conditions, which were also present in the early universe, lattice QCD calculations predict a crossover transition between the deconfined chirally symmetric phase and the confined phase with broken chiral symmetry. For high chemical potentials and low temperatures a first order chiral phase transition is expected and will be tested at the FAIR facility at GSI Darmstadt.

Due to their large central densities, compact stars can also serve as laboratories for nuclear matter beyond saturation density and may contain quark matter [1]. The formation of quark matter in compact stars is mainly discussed in two scenarios, in protoneutron stars (PNS) after the supernova explosion [2] and in old accreting neutron stars [3, 4]. For the first case, deleptonization leads to the loss of lepton pressure and therefore to an increase in the central density so that the phase transition takes place. Possible observables are the emission of gravitational waves [3, 4] due to the contraction of the neutron star or delayed γ -ray bursts [5].

In this article we want to follow a third and less discussed case. The phase transition from hadronic to quark matter can already occur in the early postbounce phase of a core-collapse supernova [6, 7, 8, 9, 10]. This requires a phase transition onset close to saturation density, which can be realized for high temperatures and low proton fractions. For such a scenario Ref. [8] found the formation of a second shock as a direct consequence of the phase transition. However, the lack of neutrino transport in their model allowed them to investigate the dynamics

only for a few ms after bounce. Very recently, a quark matter phase transition has been considered with Boltzmann neutrino transport for a 100 M_{\odot} progenitor [11]. The appearance of quark matter shortened the time until black hole formation due to the softening of the equation of state (EoS), but did not lead to the launch of a second shock.

In our core-collapse simulations of low- and intermediate-mass progenitor stars, we confirm the formation of a second shock caused by the phase transition to quark matter. We even find that the second shock triggers a delayed supernova explosion during the postbounce accretion phase. This represents an interesting addition to currently discussed supernova explosion mechanisms, such as the neutrino-driven [12], the magneto-rotational [13, 14] or the acoustic mechanisms [15]. A clear imprint of the phase transition to quark matter at the launch of the explosion could be expected in the neutrino signal, the emission of gravitational waves and the nucleosynthesis yields. Given the improvements in the sensitivity of neutrino detectors since SN1987A, it seems that the neutrino signal from a Galactic supernova is the most likely observable which could provide a first indication of the early phase transition to quark matter.

Lattice QCD is not yet able to make predictions for large chemical potentials relevant for neutron star calculations. Consequently, the quark matter EoS is currently computed using phenomenological descriptions such as the MIT bag or the NJL models. As we aim to study the basic effects from quark matter phase transitions on core-collapse supernovae, we chose the very simple but widely applied MIT bag model. In modeling the phase

transition to quark matter there is a main physical uncertainty: the critical density n_{crit} for the onset of the mixed phase. In our model, n_{crit} is determined by the bag constant B and the strange quark mass. At present, the bag constant is not a fixed parameter and is usually chosen between $B^{1/4} = 145 - 200$ MeV [16]. We choose the bag constant such that we obtain an early onset for the phase transition and a maximum mass of more than $1.44 M_{\odot}$, without enabling absolutely stable strange quark matter. Within this narrow range we select $B^{1/4} = 162$ MeV (*eos1*) and 165 MeV (*eos2*), and a strange quark mass of 100 MeV as indicated by the Particle Data Group [17]. The two choices of the bag constants lead to critical densities of $\sim 0.12 \text{ fm}^{-3}$ and $\sim 0.16 \text{ fm}^{-3}$, respectively (for $T = 0$ and proton fraction $Y_p = 0.3$). For the hadronic EoS we use the table of Shen et al. [18]. The phase transition to quark matter is modeled by a Gibbs construction as discussed in Refs. [9, 11] and is therefore of second order according to the Ehrenfest classification but a phase transition of the first kind after Landau's definition [19]. The phase diagram using *eos1* for different proton fractions Y_p is shown in Fig. 1. We remark that larger values for the bag constant result in higher critical densities. For the sake of simplicity, we have neglected finite size effects and Coulomb interactions within the mixed phase. Such contributions would decrease the density range of the mixed phase making the phase transition more similar to a Maxwell construction [20]. For comparison, we have also computed the EoS by using the Maxwell construction and find that the results of our core-collapse simulations are qualitatively similar.

We note that the small obtained values for the critical density close to saturation density are not in contradiction with heavy ion data. In contrast to heavy-ion collisions high-density supernova matter is isospin-asymmetric with a proton fraction $Y_p \sim 0.3$. Furthermore SN timescales are in the range of ms and therefore long enough to establish equilibrium with respect to weak interactions that change the strangeness on the timescales of micro-seconds or less. The additional strange quark degree of freedom and the large asymmetry energy allow one to obtain small values for n_{crit} and lead to an early appearance of quark matter (see Fig. 1).

Our choice of parameters is also compatible with the still most precise neutron star mass measurement of $1.44 M_{\odot}$ for the Hulse-Taylor pulsar [21]. With *eos1* and *eos2*, we obtain values for the maximum gravitational mass of 1.56 and $1.50 M_{\odot}$ respectively. Note that higher neutron star masses can be achieved with more sophisticated models of quark matter [22]. For $B^{1/4}=162$ and 165 MeV, almost the entire star is composed of quark matter, surrounded by a mixed quark-hadronic phase, which is enclosed by a thin pure hadronic crust.

For the accurate prediction of the three-flavor neutrino signal, general relativistic effects may be important. Hence, we choose for our investigation a well-tested

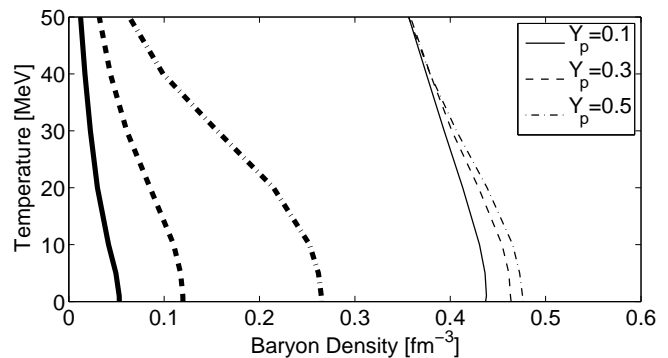


FIG. 1: The onset (thick lines) and the end (thin lines) of the mixed phase from the QCD phase transition from nuclear matter to quark matter using *eos1*.

general relativistic description of the neutrino radiation hydrodynamics in spherical symmetry, that is based on Boltzmann neutrino transport [23, 24, 25]. Quark matter appears only in optically thick regimes where neutrinos are in thermal and chemical equilibrium with matter. For this first proof-of-principle study, we use hadronic weak interaction rates [26] in the quark phase and derive the hadronic chemical potentials from the quark chemical potentials such that weak equilibrium for neutrinos in quark matter is obtained. Our simulations are launched from a 10 and a $15 M_{\odot}$ progenitor model from Ref. [27].

The standard core-collapse scenario leads to core bounce at nuclear saturation density and the formation of a shock. This expanding shock loses energy due to the dissociation of nuclei and the emission of the ν_e -burst at ~ 10 ms after bounce (see Fig. 2 (a)) and therefore turns into a standing accretion shock (SAS). The SAS could be revived by neutrino heating [12]. However, explosions in spherically symmetric models with accurate neutrino transport have only been obtained for a $8 M_{\odot}$ ONeMg progenitor star [28]. The collapse of more massive progenitors leads to an extended postbounce phase, during which the central PNS contracts due to mass accretion.

In our models that allow a transition to quark matter, the onset of the mixed phase ($n_B \sim 0.1 \text{ fm}^{-3}$, $T \simeq 10$ MeV, $Y_e \sim 0.3$) is already achieved at core bounce. The initially reached quark matter fraction at the center of the PNS remains small during the first 50 ms after bounce. In the subsequent compression, the quark matter fraction rises again and an increasing central region of the PNS enters the mixed phase. The reduced adiabatic index causes the PNS to collapse.

PNS collapse: The central density rises up to $4 - 5$ times nuclear saturation density where the collapse halts due to the stiffening of the EoS in the pure quark phase. A large fraction of the PNS is composed of quarks, enclosed by a mixed hadronic-quark phase, which is surrounded by the infalling hadronic envelope (see Table I). The mixed phase region shrinks gradually during the

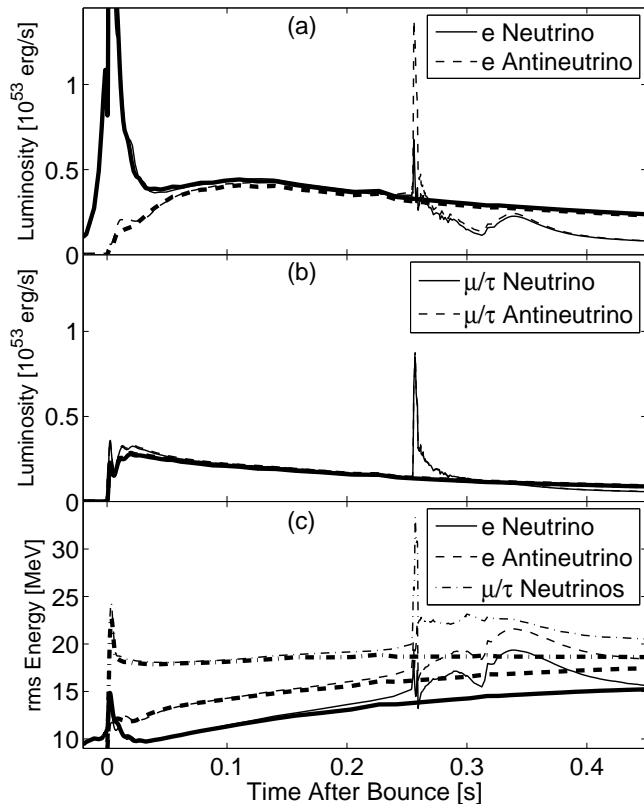


FIG. 2: Neutrino luminosities (a) and (b) and rms-energies (c) measured at 500 km distance for a $10 M_{\odot}$ progenitor model. The results of the quark EoS *eos1* (thin lines) are compared to the results of the pure hadronic EoS [18] (thick lines). A second neutrino burst is clearly visible at ~ 260 ms after bounce.

Prog.	EoS	t_{pb}	M_Q	M_{mixed}	M_{PNS}	E_{expl}
[M_{\odot}]		[ms]	[M_{\odot}]	[M_{\odot}]	[M_{\odot}]	[10^{51} erg]
10	<i>eos1</i>	255	0.850	0.508	1.440	0.44
10	<i>eos2</i>	448	1.198	0.161	1.478	1.64
15	<i>eos1</i>	209	1.146	0.320	1.608	0.42
15	<i>eos2</i>	330 ^a	1.496	0.116	1.700	unknown ^b

^amoment of black hole formation

^bblack hole formation before positive explosion energy is achieved

TABLE I: Selected properties of the different models. t_{pb} is the time after bounce at the first appearance of the pure quark phase. The different mass distributions (baryon mass) of the PNS, the quark mass M_Q , the mass of the mixed phase M_{mixed} and the total PNS mass M_{PNS} are taken at a later stage when clearly positive explosion energies E_{expl} are obtained.

PNS collapse as more and more matter converts from the mixed into the pure quark phase. On this short time scale of ~ 1 ms, the SAS remains almost unaffected by this dynamical evolution inside the PNS (see Fig. 3). However, the change in the chemical potentials and the increasing

density during the phase transition establish weak equilibrium at a lower electron fraction of $Y_e \leq 0.1$, while the mean energy of the trapped ν_e increases above 200 MeV.

Shock formation and early shock propagation: A sub-sonic accretion front forms at the interface between the hydrostatic pure quark phase and the infalling mixed phase (thick dashed line Fig. 3). The accretion front propagates through the mixed phase, meets the supersonically infalling hadrons at the sonic point and turns into an accretion shock (thick dash-dotted line). The internal energy of the infalling hadronic matter, that is accumulated on the compactified core of the PNS, increases significantly due to the compression in the strong gravitational field. This leads to a rapid conversion of hadronic matter into the mixed phase. As the accreted layers become less dense, the second accretion shock finally detaches from the mixed phase boundary and propagates into the pure hadronic phase. This phase was depleted by the continued emission of electron neutrinos after the first neutronization burst. In this electron-degenerate environment, weak equilibrium is achieved at an electron fraction ~ 0.1 . When the second shock runs across this matter, the electron-degeneracy is lifted by shock-heating and the weak equilibrium is restored at higher values of the electron fraction ($Y_e \geq 0.2$).

Explosion: As the second shock propagates through the outer layers of the PNS, the ram pressure ahead of the shock decreases rapidly due to the large decline of density and velocity. The pressure behind the shock is supported by the accumulation of the infalling shock-heated matter and the increasing electron pressure due to the larger Y_e in the adjusting weak equilibrium. Hence, this accretion shock accelerates and turns into a dynamic shock with positive matter velocities (thin solid line in Fig. 3). Up to this point, neutrino transport plays a negligible role since neutrinos are trapped. This changes when the second shock reaches the neutrino spheres. A second neutrino burst of all neutrino flavors is released (see Fig. 2), dominated by $\bar{\nu}_e$ due to the above-mentioned increase in Y_e . In addition, the more compact PNS releases (μ/τ) -neutrinos with significantly higher mean energies as illustrated in Fig. 2 (c). As soon as the expanding second shock merges with the outer SAS, the scenario resembles the situation of a neutrino-driven explosion mechanism (thin dashed line in Fig. 3), except for the large matter outflow with velocities $\sim 10^5$ km/s. Behind the expanding matter, a region with matter inflow develops due to neutrino cooling (thin dash-dotted line). The corresponding accretion luminosity from the later fallback explains the transient increase of the electron neutrino flavor luminosities in Fig. 2 (a) ~ 340 ms after bounce. This matter inflow in the cooling region becomes supersonic and develops another standing accretion shock at the surface of the PNS at a radius of ~ 50 km. The neutrinos emitted from this cooling region are partly absorbed behind the expanding shock at a few 100 km radius and support the

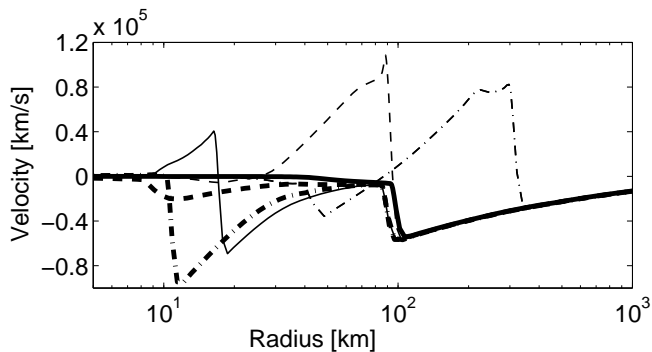


FIG. 3: Velocity profiles at different times during the post-bounce evolution of a $10 M_{\odot}$ progenitor model based on *eos1*, illustrating the development of the explosion through different stages; thick solid line at 240.5 ms, dashed at 255.2 ms, dash-dotted at 255.5 ms and thin solid line at 256.4 ms, dash-dotted at 258.3 ms.

explosion additionally. We obtain explosion energies of several 10^{50} erg (see Table I). The neutrino luminosities decrease after the onset of the explosion (see Fig. 2 at ~ 350 ms after bounce).

In general, the models with *eos1* and *eos2* evolve in a qualitatively similar manner. However, the models with the larger bag constant show a longer PNS accretion time before the onset of the phase transition due to the larger critical density. This results in a more massive PNS with a deeper gravitational potential, so that the second shock develops larger explosion energies (see Table I). In comparison to the simulations using *eos1*, the second neutrino burst appears several 100 ms later and is found to have a larger peak-luminosity due to higher temperatures of the shocked material. The more massive progenitor stars give an earlier onset of the phase transition and result in a more massive PNS. A special case is the dynamical evolution of the PNS of the $15 M_{\odot}$ progenitor model using *eos2*. Almost simultaneously with the formation of the second shock, the more compact quark core collapses to a black hole. Still, this does not necessarily exclude an explosion. Unfortunately, our co-moving coordinate choice does not allow us to follow the dynamical evolution beyond the formation of the apparent horizon [25].

The main result of this investigation is a strong signature of the formation of quark matter in the early postbounce phase of core collapse supernovae. A second shock forms inside the PNS, that affects significantly the properties of the emitted neutrinos. For a Galactic core-collapse supernova, a second neutrino burst should be resolvable by the present neutrino detectors. Unfortunately, the time sequence of the neutrino events from SN1987a [30] was statistically not significant. Anyway, the goal of this first study is to predict the general effects of the early phase transition to quark matter during the postbounce phase. To optimally reproduce the ob-

servations from SN1987A further analysis and improvements of the EoS would be required. The magnitude and the time delay of the second neutrino burst provide correlated information about the critical density, the EoS in different phases and the progenitor model. For low and intermediate mass progenitor models, the energy of the second shock becomes sufficient to drive an explosion even in spherical symmetry. The explosion is powered by the accretion of matter into the deeper gravitational potential of the more compact PNS, if quark matter is present in the core. The ejecta contain neutron-rich material that expands on a fast timescale and should be investigated as a possible site for the r-process. With respect to the remnant, the narrow range of PNS masses found in Table I may provide an explanation for the clustering of the observed neutron star masses (gravitational) around $1.4 M_{\odot}$ (see e.g. [21]). The discussed direct black hole formation at the phase transition could be investigated further in light of the observed connection between supernovae and γ -ray bursts [31]. For other progenitor models, a delayed collapse to a black hole may occur after the explosion during the PNS cooling phase.

The presented analysis should be complemented by multi-dimensional simulations, to explore the impact of known fluid instabilities that can not be treated in spherical symmetry. Another interesting scenario would be a weak neutrino driven explosion, followed by a fallback-induced QCD phase transition. Since the QCD phase diagram shows a large variety of color-superconducting phases [32, 33, 34], a more sophisticated quark matter EoS should be adopted. This could lead to a second phase transition within the quark core of the PNS and would be an interesting extension of the present study.

This work has been supported by the Swiss National Science Foundation under the grant numbers PP002-106627/1 and PP200020-105328/1, the Helmholtz Research School for Quark Matter Studies, the Italian National Institute for Nuclear Physics, the Frankfurt Institute for Advanced Studies and by the ESF CompStar program. A.M. is supported at the Oak Ridge National Laboratory, which is managed by UT-Battelle, LLC for the U.S. Department of Energy under contract DE-AC05-00OR22725. We would like to thank for stimulating discussions with D. Blaschke, A. Drago, G. Martínez-Pinedo and S. C. Whitehouse.

-
- [1] F. Weber, Progress in Particle and Nuclear Physics **54**, 193 (2005).
 - [2] J. A. Pons, A. W. Steiner, M. Prakash and J. M. Lattimer, Phys. Rev. Lett. **86**, 5223 (2001).
 - [3] L.-M. Lin, K. S. Cheng, M. C. Chu and W. M. Suen, Astrophys. J. **639**, 382 (2006).
 - [4] E. B. Abdikamalov, H. Dimmelmeier, L. Rezzolla and J. C. Miller (2008), astro-ph/0806.1700.

- [5] Z. Berezhiani, I. Bombaci, A. Drago, F. Frontera and A. Lavagno, *Astrophys. J.* **586**, 1250 (2003).
- [6] M. Takahara and K. Sato, *Astrophys. J.* **335**, 301 (1988).
- [7] M. Takahara and K. Sato, *Progress of Theoretical Physics* **80**, 861 (1988).
- [8] N. A. Gentile, M. B. Aufderheide, G. J. Mathews, F. D. Swesty, and G. M. Fuller, *Astrophys. J.* **414**, 701 (1993).
- [9] A. Drago and U. Tambini, *J. Phys.* **G25**, 971 (1999).
- [10] N. Yasutake, K. Kotake, M.-a. Hashimoto, and S. Yamada, *Phys. Rev.* **D75**, 084012 (2007).
- [11] K. Nakazato, K. Sumiyoshi, and S. Yamada, *Phys. Rev.* **D77**, 103006 (2008).
- [12] H. A. Bethe and J. R. Wilson, *Astrophys. J.* **295**, 14 (1985).
- [13] J. M. LeBlanc and J. R. Wilson, *Astrophys. J.* **161**, 541 (1970).
- [14] G. S. Bisnovatyi-Kogan, *Soviet Astronomy* **14**, 652 (1971).
- [15] A. Burrows, E. Livne, L. Dessart, C. D. Ott and J. Murphy, *New Astronomy Review* **50**, 487 (2006).
- [16] K. Schertler, C. Greiner, J. Schaffner-Bielich, and M. H. Thoma, *Nucl. Phys.* **A677**, 463 (2000), [astro-ph/0001467](#).
- [17] S. Eidelman et al. (Particle Data Group), *Phys. Lett.* **B592**, 1 (2004).
- [18] H. Shen, H. Toki, K. Oyamatsu and K. Sumiyoshi, *Nucl. Phys.* **A637**, 435 (1998).
- [19] L. D. Landau and E. M. Lifshitz, *Statistical physics. Pt.1* (Course of theoretical physics - Pergamon International Library of Science, Technology, Engineering and Social Studies, Oxford: Pergamon Press, and Reading: Addison-Wesley, —c1969, 2nd rev. - enlarg.ed., 1969).
- [20] D. N. Voskresensky, M. Yasuhira and T. Tatsumi, *Nucl. Phys.* **A723**, 291 (2003).
- [21] J. M. Lattimer and M. Prakash, *Science* **304**, 536 (2004).
- [22] M. Alford et al., *Nature* **445**, E7 (2007).
- [23] A. Mezzacappa and S. W. Bruenn, *Astrophys. J.* **410**, 740 (1993).
- [24] A. Mezzacappa and O. E. B. Messer, *Journal of Computational and Applied Mathematics* **109**, 281 (1999).
- [25] M. Liebendörfer, O. E. B. Messer, A. Mezzacappa, S. W. Bruenn, C. Y. Cardall, and F.-K. Thielemann, *Astrophys. J. Supplement* **150**, 263 (2004).
- [26] S. W. Bruenn, *Astrophys. J. Supplement* **58**, 771 (1985).
- [27] S. E. Woosley, A. Heger and T. A. Weaver, *Reviews of Modern Physics* **74**, 1015 (2002).
- [28] F. S. Kitaura, H.-T. Janka, and W. Hillebrandt, *A&A* **450**, 345 (2006).
- [29] A. Steiner, M. Prakash and J. M. Lattimer, *Phys. Lett.* **B486**, 239 (2000).
- [30] K. S. Hirata, T. Kajita, M. Koshiba, M. Nakahata, Y. Oyama, N. Sato, A. Suzuki, M. Takita, Y. Totsuka, T. Kifune, et al., *Phys. Rev. D* **38**, 448 (1988).
- [31] T. Piran, *Reviews of Modern Physics* **76**, 1143 (2005).
- [32] S. B. Rüter, V. Werth, M. Buballa, I. A. Shovkovy, and D. H. Rischke, *Phys. Rev. D* **72**, 034004 (2005).
- [33] D. Blaschke, S. Fredriksson, H. Grigorian, A. M. Öztaş, and F. Sandin, *Phys. Rev. D* **72**, 065020 (2005).
- [34] F. Sandin and D. Blaschke, *Phys. Rev.* **D75**, 125013 (2007), [astro-ph/0701772](#).